Effect of melt spinning on the integrity of poly(ether ether ketone) for commingled yarn based composite preforms

Lisa Feuillerat, Olivier de Almeida, Jean-Charles Fontanier, Carole Aubry, Pascal Rumeau, Fabrice Schmidt

Effect of melt spinning on the integrity of poly(ether ether ketone) for commingled yarn based composite preforms

Lisa Feuillerat[a,*], Olivier De Almeida[a], Jean-Charles Fontanier[b], Carole Aubry[b], Pascal Rumeau[b], Fabrice Schmidt[a]

[a] Institut Clément Ader (ICA), Université de Toulouse, CNRS UMR 5312, IMT Mines Albi, UPS, INSA, ISAE-SUPAERO, Campus Jarlard, Albi F-81013, France
[b] Institut Francais du Textile et de l'Habillement (IFTH), 14 Rue des Reculettes, F-75013 Paris, France

A B S T R A C T

PEEK yarns are used for commingled yarn based preforms in order to manufacture high performance thermoplastic composites. In a previous work, characterizations of PEEK commingled yarns revealed degradation, causing poor consolidation of final composites. The sizing applied onto the yarn surface in the melt spinning was identified as a degradation factor. Thus, the aim of this work is to assess the effect of different melt spinning parameters: extrusion, sizing and draw ratio, on PEEK integrity and its degradation process. Yarns at different stages of melt spinning were characterized through various techniques. For all yarns, degradation was identified during further transformation, in the molten state, inducing a decrease of the crystallization temperature and an increase of viscosity due to crosslinking. Extrusion initiates degradation earlier without changing the PEEK decomposition process. Sizing is responsible for an acceleration and modifications of degradation steps.

Keywords:
PEEK
Thermal oxidation
Crosslinking
Melt spinning
Sizing

1. Introduction

Poly(ether ether ketone) (PEEK) is increasingly used as matrix for high performance composites because of its thermo-mechanical stability and its chemical resistance [1]. PEEK can be used up to a peak service temperature of 200 °C thanks to its glass transition and melting temperatures respectively of 143 °C and 343 °C.

However, the processing of such heat-stable matrix composites is a major difficulty due to the high molten viscosity of PEEK [2]. To overcome this difficulty, manufacturers have developed preforms to reduce the distance the matrix has to travel to impregnate the reinforcements. The main solutions proposed are preimpregnated tapes, powdered fabrics, film stacking, cowoven fabrics and commingled yarns, which are generally consolidated by thermo-compression.

Preimpregnated tapes consist of reinforcements previously embedded in a thermoplastic matrix, such as the commercial product AS4/APC-2, a PEEK tape reinforced with unidirectional carbon fiber. This solution provides good interfacial bonding, but the manufacturing of complex shapes is difficult due to its stiffness [3]. Powdered fabrics, as the name suggests are fabrics covered by a PEEK powder melted to wet reinforcements. Homogeneous dispersion and sufficient adhesion of PEEK with reinforcements are the main difficulties of powdered fabrics. Another solution is to stack polymer films with reinforcement fabrics, but the difficulty is to force the polymer flow through reinforcements made of thousands of filaments. Furthermore, this solution does not allow the production of complex geometries [4]. The matrix can also be cowoven into a fabric, where reinforcements and matrix yarns are combined as warp and weft yarns, but this leads to a heterogeneous distribution. Finally, the commingled yarns are the most interesting solution with an intimate contact and therefore an excellent dispersion between the reinforcement and the matrix [5].

However, as shown in a previous publication, unacceptable void contents of about 10% are obtained when consolidating commingled yarn based products involving a PEEK matrix [6]. The main reason of such behavior is a rapid thermal degradation of PEEK, in the range of processing temperature beyond 380 °C. As widely studied in the literature, in the molten state, PEEK is subjected to degradation [7–15]. Firstly chain scission occurs at ether or ketone bonds, then oxidation takes place and leads to the formation of hydroperoxides and other degradation products, which finally leads to crosslinking [16,17]. This degradation process induces significant changes of the thermal, rheological and mechanical properties of PEEK, such as a decrease of the crystallization and melting temperatures, an increase of its viscosity, glass transition temperature,

* Corresponding author.
E-mail address: lisa.feuillerat@mines-albi.fr (L. Feuillerat).

and molecular weight. The degradation of the PEEK matrix in the molten state has been characterized at different scales and the rapid increase of its viscosity makes impossible the impregnation and consolidation of such architecture made of commingled yarns.

The previous study has shown that the initial state of the PEEK yarns is responsible for the acceleration of PEEK degradation and thus the impossibility to consolidate this commingled yarn based preform [6]. Indeed, a first processing step is achieved in order to prepare commingled yarn based preforms: the melt spinning operation to obtain PEEK yarns. During this process, PEEK is melted and extruded through a spinneret leading to a multifilament yarn. In order to prevent breakage, friction and electrostatic effect, a specific solution, called sizing is applied onto the surface of yarns before drawing and winding. Sizing has been identified as a factor responsible for degradation by accelerating it during the further processing of the commingled yarn based preform, in the molten state. Therefore, the manufacturing of PEEK yarns is a crucial processing step that can be critical for the consolidation of composites, as it is carried out at high temperature, under high mechanical stress and requires additives that induce an initial degradation of the PEEK matrix.

However, although yarn sizing has been identified to have an effect on PEEK degradation, the extrusion and drawing may also have a critical effect on the PEEK stability. Thus, this paper aims to determine, through various experimental analyses, the influence of different melt spinning parameters on the stability, thermal and rheological properties of poly(ether ether ketone) and its degradation process. In order to evaluate the consequences of melt spinning on the integrity of PEEK, yarns were collected at different stages of the melt spinning process, characterized and compared to the properties of raw PEEK.

2. Experimental

2.1. Materials

The raw PEEK polymer was processed by melt spinning at 390 °C. This process is composed of different equipments which are schematically shown in Fig. 1. The raw material in pellets form is melted through the extruder and the molten polymer flows through a spinneret. The spun filaments are then drawn in the molten state while cooled in the cooling chamber, and a sizing is sprayed onto the surface of yarns. The filaments are then guided over godets heated above the glass transition temperature and finally wound up.

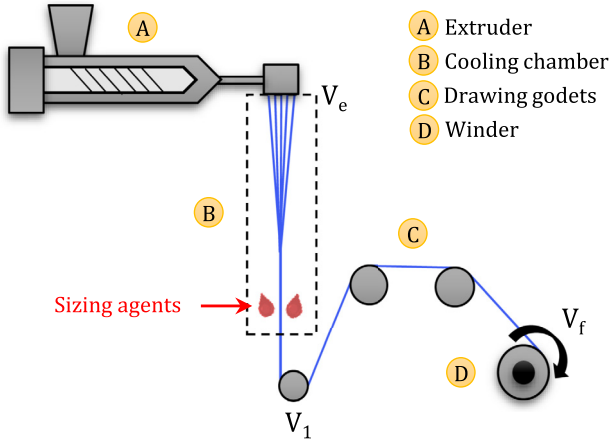

Fig. 1. Schematic of the melt spinning process.

Table 1
Name and sampling zone for the different yarns (DR: Draw ratio).

Sampling zone	Name	Sizing
B	Extruded yarn	–
D	Drawn yarn $DR = 1$	Yes
D	Drawn yarn $DR = 2$	Yes
D	Drawn yarn $DR = 3.75$	Yes

A drawing stage takes place between the first and the last godet. This draw ratio (DR) is defined as the ratio between the speed of rotation of the last godet (V_f) and that of the first godet (V_1), as described in the Eq. (1).

$$DR = \frac{V_f}{V_1} \tag{1}$$

In this study, the spinneret was composed of 48 holes of 0.4 mm and the sizing used was made up mainly of fatty acid ester and poly(ethylene-glycol) ester. The resulting sizing ratio was 1.5% in mass. The same extrusion flow rate was applied in order to obtain filaments of the same diameter for all yarns. Then, various yarn samples were collected at different stages of the process, as summarized in Table 1. The first yarn, referred to as extruded yarn, was collected right after extrusion in the cooling chamber before being sized and drawn, the other yarns were collected at the end of the melt spinning process after being impregnated with sizing. The latter are referred to as drawn yarns $DR = 1$, $DR = 2$, $DR = 3.75$. The drawn yarns $DR = 1$ correspond to the yarns obtained with all godets at the same speed of rotation. The drawn yarns $DR = 2$ and $DR = 3.75$ correspond to yarns that were drawn with a faster rotational speed of the last godet equal to 2 and 3.75 times that of the first godet respectively.

In order to avoid morphological effects during characterizations, the filaments were ground using a Retsch ultra centrifugal mill ZM 100 with a 0.5 mm sieve. The mill was cooled with liquid nitrogen to avoid overheating. The powders obtained were then characterized through different analyses.

2.2. Thermogravimetric analysis

The thermal degradation was studied by means of thermogravimetric analysis (TGA) with a Setsys SETARAM TGA. About 20 mg of each sample was first held at 100 °C for 15 min, and then heated to 800 °C at a heating rate of 10 °C min^{-1}, under argon. In order to check the repeatability, the test was reproduced 3 times. The temperature related to a 5% weight loss ($T_{5\%}$) was taken to compare the samples.

2.3. Differential scanning calorimetry

Differential scanning calorimetry (DSC) was achieved in order to evaluate the evolution of thermal properties in the molten state with a power-compensated Perkin Elmer 8500 DSC. For all experiments, aluminum sealed pans filled with 3.7 ± 0.02 mg of sample were used. The samples were subjected to four heating and cooling cycles in a nitrogen atmosphere between 50 and 400 °C. The thermal treatment consisted in heating the sample at 20 °C min^{-1} until 400 °C, then in applying an isotherm at this temperature for 20 min, and finally in cooling the sample with a constant rate of 10 °C min^{-1} to induce PEEK crystallization in identical conditions. The first one was applied to erase the thermal history and the isotherm at 400 °C was only 5 min. As explained by Jonas et al. [10], above 385 °C, self-nucleation is eliminated and starting from 400 °C, thus ensured starting crystallization from a free-nuclei melt. During the last stage of the thermal treatment, the crystallization temperature (T_c) was measured. For convenience,

the T_c was taken at the maximum heat flow of the crystallization exothermic peak. Identical trends on the T_c were obtained by taking the peak onset as a reference for T_c. Nevertheless, the results were much more scattered. In order to check the repeatability, the test was reproduced 3 times.

2.4. Rheometry

The evolution of the melt viscosity was also studied in order to assess the effect of the melt spinning transformation on the degradation kinetics of PEEK. The samples were prepared with the same method to avoid morphological effects. The powders were compacted with a force of 29 kN during 1 min using an Instron press 5567 and a cylindrical die with a diameter of 20 mm. The resulting tablets were then consolidated in a press using a pilot plant for thermo-compression molding process equipped with the 3iTechë technology from Roctool. The applied thermo-compression cycle consisted of a heating phase at 42 °C min^{-1}, a 3 min isothermal step at 370° under a force of 125 kN, and finally in a cooling stage at 50 °C min^{-1}.

Rheological measurements were performed on these consolidated samples with a Mars Haake rheometer using a plate-plate geometry in oscillatory mode with 20 mm diameter disposable aluminum plates. In order to check the repeatability, the test was reproduced 3 times. The heating conditions were optimized so as to get the fastest heating rate without a temperature overshoot higher than 1 °C. This strategy was selected for limiting the exposure time of PEEK to an oxidant atmosphere once melted, which in turn may generate temperature differences within the sample during the several tens of seconds. During the isothermal experiments at 400°, constant shear and shear rates of 0.01 and 6.28 S^{-1} (Hz) respectively were applied. In order to guarantee the linear viscoelastic range, strain sweep tests were carried out beforehand so that the complex viscosity could be determined simply from the elastic and viscous moduli G_S and G_L.

2.5. Thermogravimetric analysis coupled to Fourier transform infrared spectroscopy

Thermogravimetric analysis coupled to Fourier Transform Infrared Spectroscopy (TGA-FTIR) was performed using a NETZSCH 209F1 Iris instrument. The samples were first held at 100 °C for 15 min, and then heated to 800 °C at a heating rate of 10 °C min^{-1} under nitrogen. The emitted gases were analyzed with a BRUKER Tensor 27 FTIR. The spectra were collected with an acquisition frequency of 6 spectra per minute and the measurements were performed with a resolution of 4 cm^{-1}. In order to check the repeatability, the test was reproduced 3 times.

2.6. Pyrolysis-gas chromatography–mass spectroscopy/flame ionization detector

Analytical pyrolysis was carried out in a micropyrolysis unit (Multi-shot pyrolyzer Model EGA/PY 3030D). This device was coupled to a gas chromatograph (GC, Agilent 8890 Gas Chromatograph) equipped with a mass spectrometry (Agilent 5977 Series MSD System) and a flame ionization detector (FID). Approximately 0.2 mg of the sample was placed in a steel cup and weighted with a micro-balance. The cup was loaded into the multi-shot sampler of the micro-pyrolysis unit. A heating rate of 56 °C min^{-1} was applied until reaching 600 °C under a helium flow of 120 mL min^{-1}. Volatile compounds were separated and analyzed with a GC–MS/FID system using a HP-5MS column (length 30 m; internal diameter 0.25 mm; film thickness 0.25 μm, Agilent Technologies, USA). The injector temperature was kept at 300 °C. The initial GC oven temperature was 50 °C, heated to 200 °C at 2 °C min^{-1} and then to 320 °C at 3 °C min^{-1}. Peak identification of chromatograms was achieved using the NIST (2017) mass spectral library.

3. Results and discussion

3.1. Thermal stability of raw material and yarns

The thermogravimetric results obtained in non-isothermal conditions (10 °C min^{-1}) under argon atmosphere are presented in Fig. 2. The temperature related to a weight loss of 5% ($T_{5\%}$) are also summarized in Table 2. Three groups of data can be distinguished: the sizing, the sized drawn yarns and the extruded yarn with the raw material.

The sizing has a lower thermal stability compared with the PEEK samples, with a first intense weight loss below 100 °C. This first decrease of weight correspond to a weight loss of 5% at around 88 °C. It is due to the evaporation of the sizing solvent. The second intense weight loss around 300 °C can be related to the degradation of fatty acid ester and poly(ethylene-glycol) ester, which are the sizing compounds.

In the melt spinning process, sizing is applied to the PEEK yarn before the yarns being drawn at a temperature of 170 °C. Thus, the volatile compounds of the sizing are evaporated and only the fatty phase remains on the yarn. This fatty phase, corresponding to the dry sizing, remains stable until 300 °C. In this sense, the stability of sizing must be evaluated with regard to the process, i.e. in the dry state. Thus, the temperature related to a mass loss of 5% for the dry sizing is about 316 °C.

An intense degradation phenomenon is observed for the raw material with a maximum intensity at around 574 °C. This degradation is directly linked to random chain scissions between aromatic rings and ether or ketone bonds [18]. The same behavior can

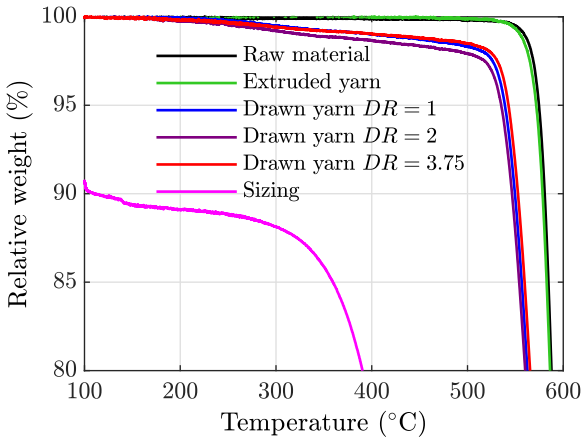

Fig. 2. TGA of all samples, performed in neutral atmosphere with a heating rate of 10 °C min^{-1}.

Table 2
Temperature related to a weight loss of 5% ($T_{5\%}$) and uncertainty.

Sample	$T_{5\%}$ (°C)
Raw material	579 ± 3
Extruded yarn	574 ± 2
Drawn yarn $DR = 1$	544 ± 3
Drawn yarn $DR = 2$	540 ± 3
Drawn yarn $DR = 3.75$	545 ± 2
Sizing	88 ± 3
Dry Sizing	316 ± 3

be noticed for the extruded yarn. This suggests that the extrusion seems to have no significant effect on the thermal stability of PEEK.

On the contrary, the drawn yarns have a different behavior with degradation starting at around 300 °C. The relative weight decreases gradually until an intense degradation at about 539 °C, 535 °C and 542 °C respectively for the drawn yarns $DR = 1$, $DR = 2$ and $DR = 3.75$. A decrease of about 35 °C is observed for the $T_{5\%}$ compared with the raw material.

Extrusion does not seem to be the parameter responsible for this acceleration of degradation because this phenomenon is not observed on the extruded yarn. At this stage, either the sizing or the draw ratio above the glass transition could be responsible for this phenomenon. When comparing the different drawn yarns, it appears that the draw ratio (DR) seems to have no significant effect on the thermal stability of yarns. The last parameter is the presence of sizing agents on the surface of yarns. In this way, it seems that the sizing has a more significant effect on the thermal stability of PEEK. The gradually weight loss of the drawn yarns from 300 °C may be related to the degradation of the sizing.

3.2. Thermal and rheological properties of raw material and yarns

In order to assess the influence of the melt spinning transformation on the thermal and rheological properties of the different samples, DSC and rheometry analyses were carried out.

The DSC analysis consisted in applying four heat treatments at 400 °C during 20 min in order to induce progressive degradation. An example of the evolution of crystallization peaks over the heat treatment cycles is presented in Fig. 3. These exothermic peaks were recorded after melting the polymer, when cooling the sample at 10 °C min^{-1}. For both samples, the sharp peak in the first cycle broadens over the heat treatment cycles, shifting the peak maximum to lower temperatures. This effect is related to crosslinking, which induces a lower molecular mobility of chains, therefore a decrease in the crystallization ability of the polymer and the existence of a large amount of degraded polymer that crystallizes at a slower rate [8,10].

The crystallization peak of the raw material is slightly shifted towards lower temperatures as the number of heat treatment cycles increases, from about 304 °C at the first cycle to about 302 °C at the last cycle. For the drawn yarns, this shift is more pronounced, from about 300 °C in the first cycle to about 287 °C in the last cycle.

The evolution of T_c over heat treatment cycles for all samples is presented in Fig. 4. The crystallization temperature (T_c) was measured at the maximum heat flow of the exothermic peak during the cooling ramp at 10 °C min^{-1}. On one hand, it can be noticed that for all samples, the T_c decreases with the number of cycles. On the other hand, this phenomenon is increased after transformation of PEEK into yarns.

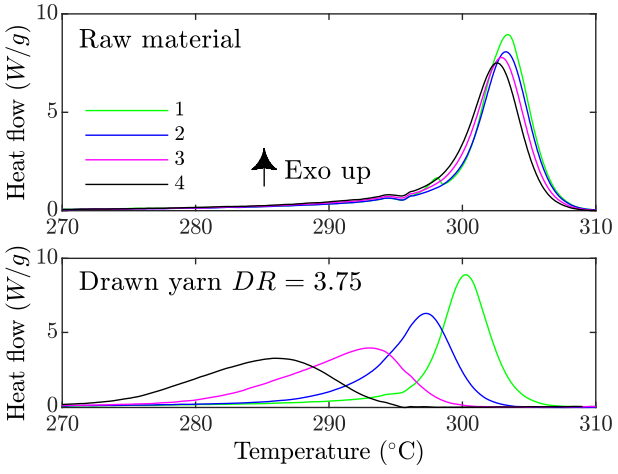

Fig. 3. Evolution of the crystallization peak during cycles at 400 °C during 20 min, under neutral atmosphere, for all samples.

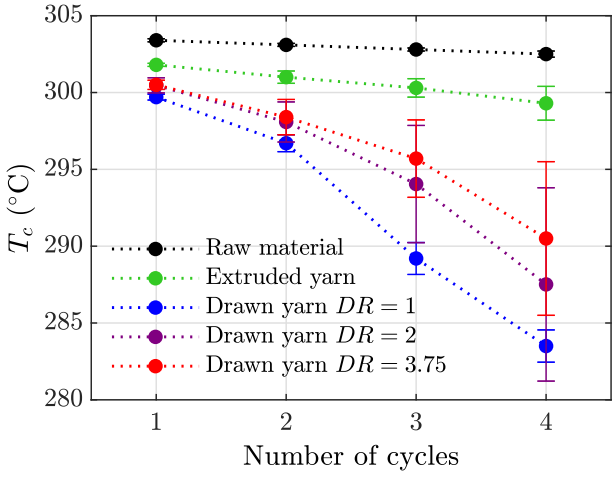

Fig. 4. Temperature of crystallization (T_c) against the number of cycles at 400 °C during 20 min, under neutral atmosphere, for all samples. Error bars are representing standard deviations.

After extrusion, a 2 °C decrease in T_c compared to the raw material is observed from the first cycle. Then the gap between the raw material and the extruded yarn increases with the number of cycles.

In the case of the drawn yarns, the T_c is 4 °C lower than that of the raw material in the first cycle, then the crystallization temperature drops over the heat treatment cycles. The final T_c is about 16 °C lower than that of the raw material.

Thus, it appears that the melt spinning transformation induces an acceleration of PEEK degradation in the molten state, on one hand due to the extrusion and on the other hand due to the sizing. These two factors therefore affect the crosslinking kinetics that cause the evolution of the crystallization behavior of PEEK. Extrusion is sufficient to accelerate the degradation. In this study, the level of degradation resulting from extrusion corresponds to a residence time in the extruder of about 10 min and an extrusion temperature of 390 °C. The effect of sizing on the crystallization temperature is even more pronounced and seems to be additional to that of extrusion.

The classification of drawn materials according to T_c suggests that a low draw ratio favors the degradation of PEEK: the higher the draw ratio, the lower the degradation. However, the sizing rate measured by Soxhlet extraction (see [6] for details) also appears to be affected by the draw ratio. It appears that the lowest sizing rate is measured on yarns of lower degradation. As the sizing conditions of the yarns are identical, this difference in sizing rate may be due to the mechanical and chemical interactions of the sized yarns at the rubbery state on the drawing godets. This effect of sizing rate on degradation kinetics has been observed in a previous study on the effect of additives on PEEK degradation [19]. Therefore, although variations in the draw ratio may affect degradation, the differences in crystallization temperature are likely to be the consequence of a difference in sizing ratio.

The evolution of viscosity with time at 400 °C under air atmosphere is presented in Fig. 5. Viscosity rapidly increases in an exponential way due to degradation for all materials. In addition to reducing the ability of polymer to crystallize, crosslinking also results in a significant increase in viscosity, similarly to that of a thermoset during curing [12,14,20].

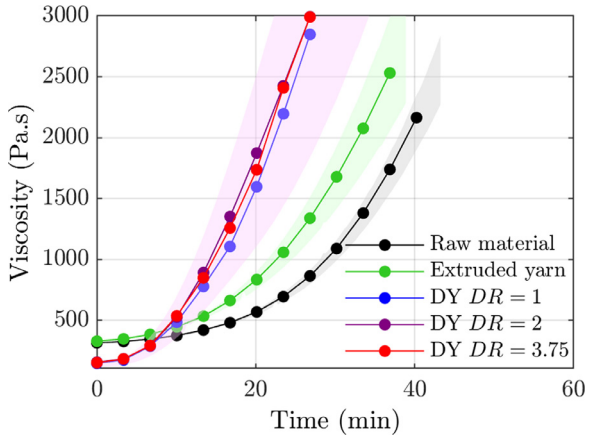

Fig. 5. Viscosity against time at 400 °C under air atmosphere for all samples. DY: Drawn yarn. Color halos are representing minimum and maximum values.

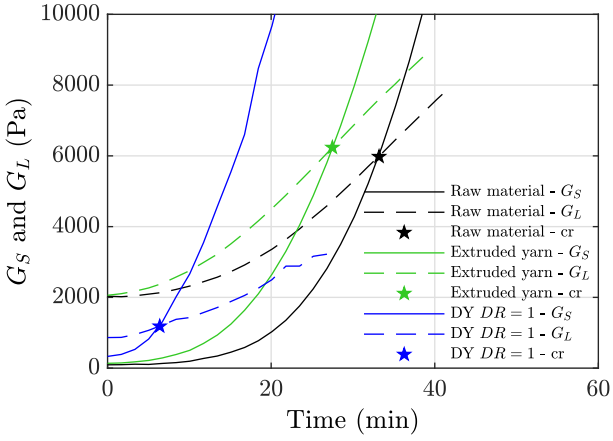

Fig. 6. Storage and loss moduli (G_S and G_L) against time during an isotherm at 400 °C under air atmosphere for all samples. DY: Drawn yarn. For clarity, the drawn yarns $DR = 2$ and $DR = 3.75$ are not shown in this figure because they are superimposed on the drawn yarns $DR = 1$.

The extruded yarn has the same initial viscosity as the raw material but the viscosity increases more rapidly. In 20 min, the viscosity of the raw material doubles whereas it almost triples for the extruded yarn.

The drawn yarns have a lower initial viscosity than the raw material and the extruded yarn. It seems that the sizing has a lubricating effect. This could be a beneficial factor in the processing of composites, as a lower viscosity facilitates the impregnation of fibrous reinforcements. However, this effect is very short lasting and the sudden increase in viscosity that follows can be disastrous for further processing of the composite like welding or hot stamping.

Finally, the same conclusion is obtained as in the DSC results, the melt spinning transformation has a huge effect on the degradation kinetics of PEEK. The time at the cross point between the storage and the loss moduli confirms also the acceleration of the degradation kinetics (Fig. 6). The loss modulus (G_L) is higher than the storage modulus (G_S) at the early stage of the experiments but with degradation, a faster increase of G_S compared to G_L occurs, leading to a crossover point that can be considered as a gel point. The crossover time between G_S and G_L has been analyzed by Chan et al. [21]. They actually noticed that the lower is the crossover time, the higher is the rate of crosslinking and therefore the gel content in the polymer. The crossover times of the different samples are summarized in Table 3. It appears that the drawn yarns, regardless of their draw ratio, have the same crossover time, which

Table 3
Crossover time (t_{cr}) between G_S and G_L, during rheometry tests at 400 °C, under air atmosphere and uncertainty.

Sample	t_{cr} (min)
Raw material	33 ± 0.9
Extruded yarn	26 ± 1
Drawn yarns	7 ± 0.6

Table 4
Molecules associated with the absorption bands of FTIR spectra.

Molecules	Absorption bands (cm^{-1})
Carbon dioxide	2358 + 2310
Carbon monoxide	2179 + 2113
Phenol	3648, 1601, 1490, 1339, 1249, 1185 and 748
Aromatic ethers	1600, 1493 and 1233
Carboxylic acid esters	2930, 2861, 1745, 1461, 1367, 1237, 1135, 965 and 720
Carboxylic acid anhydrides	1770

is considerably less than that of the extruded yarn and the raw material. In other words, the gel point is reached more quickly for the drawn yarns than the extruded yarns and the raw material.

The DSC and rheological results show that extrusion and sizing are the main factors that are responsible for an acceleration of the PEEK degradation in the molten state. Since extruded (non-sized) yarns degrade less quickly than drawn (and sized) yarns, the effect of sizing seems to be predominant over that of extrusion process. In addition, the draw ratio induces different sizing ratio leading to different degradation kinetics. This effect was identified in DSC but not by rheological analysis.

These results are in good agreement with the recent literature on poly(aryl ether ketone) (PAEK) degradation [15,19,22]. However, the physico-chemical process that results in an acceleration of the degradation kinetics has never been analyzed and was therefore further investigated in this study. In particular, the way in which the different melt spinning parameters affect the degradation process of PEEK has been analyzed.

3.3. Thermal degradation process of raw material and yarns

Thermogravimetric analysis coupled to Fourier Transform Infrared Spectroscopy (TGA-FTIR) and pyrolysis-Gas Chromatography coupled to Mass Spectroscopy and Flame Ionization Detector (py-GC–MS/FID) were used to probe the effect of extrusion, sizing and draw ratio on the PEEK degradation process.

FTIR analysis were carried out upon heating in TGA, in order to characterize the gases formed during the degradation of the different samples. FTIR spectra of the emitted gases at different temperatures during the heating stage are presented in Fig. 7. The main molecules identified and their related absorption bands are summarized in Table 4.

For the raw material, the evolution of the FTIR spectra with temperature shows the appearance of intense absorption bands attributed to phenol, carbon dioxide, carbon monoxide and aromatic ethers. These molecules are characteristic of the PEEK degradation [16,17].

The degradation by-products of the extruded and drawn yarns, whatever the draw ratio, have the same chemical nature as the raw material. However, the absorption bands characteristic of sizing degradation products (carboxylic acid esters and anhydrides) are not detected. The low proportion of sizing on the extruded yarns can explain the absence of sizing by-products, but it can also be the consequence of some interaction of those chemicals with PEEK material.

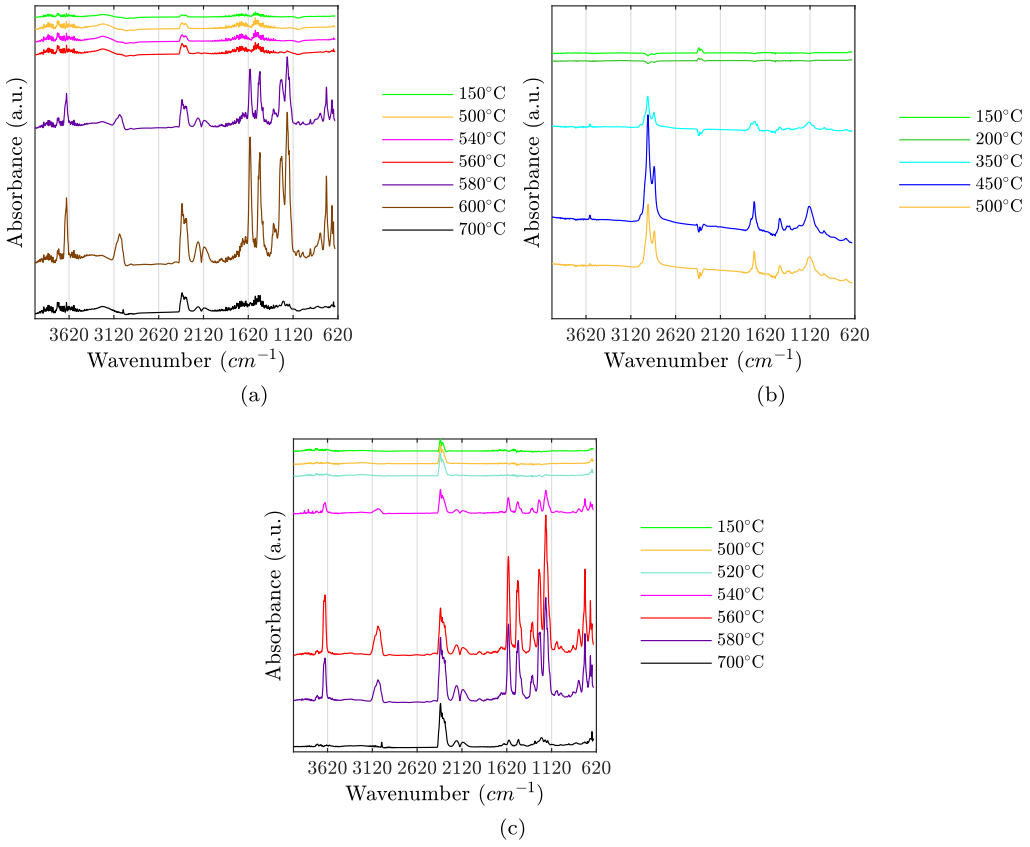

Fig. 7. FTIR spectra of emitted gases during TGA at 10 °C min^{-1}, performed in neutral atmosphere. (a) Raw material and extruded yarn, (b) Sizing (c) Drawn yarns.

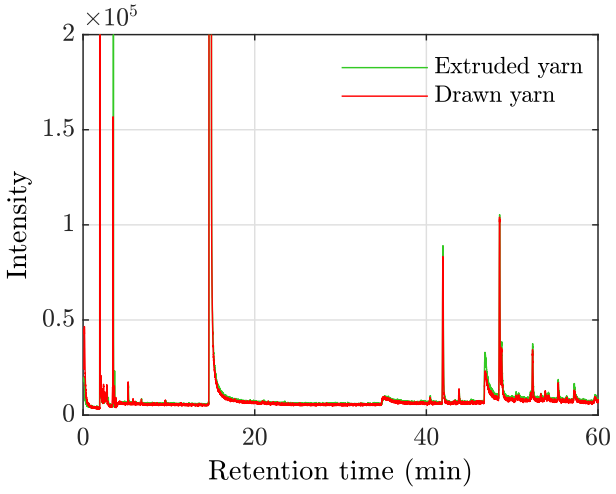

Fig. 8. Chromatograms of extruded and drawn yarns.

These observations are confirmed by py-GC–MS/FID analysis. As presented in Fig. 8, the chromatograms of the extruded and drawn yarns are perfectly superimposed. The same degradation products are formed as the same retention times in the column are observed between the extruded and drawn yarns. The separated species were then analyzed by Mass Spectroscopy and Flame Ionization Detector (MS/FID) in order to identify the related molecules, as summarized in Table 5. These degradation products detected are consistent with those identified in the literature [16]. No additional peaks were observed, thus no new species were identified. These chromatograms were also compared to the sizing chromatogram and no common peaks were identified.

Table 5
Molecules identified by MS/FID with the related retention time of chromatogram peaks.

Molecules	Retention time (min)
Carbon dioxide	3
Benzene	3.5
Toluene	5.2
Phenol	14.9
Diphenyl ether	41.9
Dibenzofuran	48.5
2-phenylphenol	48.7
Fluorene	52.3
Benzophenone	55.3
4-phenoxyphenol	60.9

Although all yarns have the same chemical nature, with the same emitted gases during the degradation, they do not have the same degradation kinetics. Indeed, as illustrated in Fig. 7 the absorption bands of the by-products appear at a lower temperature for the drawn yarns (about 540 °C), compared with the raw material and the extruded yarn (about 580 °C).

In order to highlight this acceleration of degradation, Fig. 9 shows the absorbance profiles of specific bands corresponding to the main degradation products of PEEK (phenol, carbon monoxide and carbon dioxide). This allows monitoring the evolution of the degradation process.

The comparison of the different absorbance peaks for PEEK-based materials indicates that phenol and carbon dioxide have the highest intensity and are therefore the main degradation products, which is in agreement with the literature [16,23]. Furthermore, all these products appear in the same range of temperature. For the absorption band related to phenols, a unique peak is observed contrary to that of carbon monoxide and carbon dioxide, which exhibit

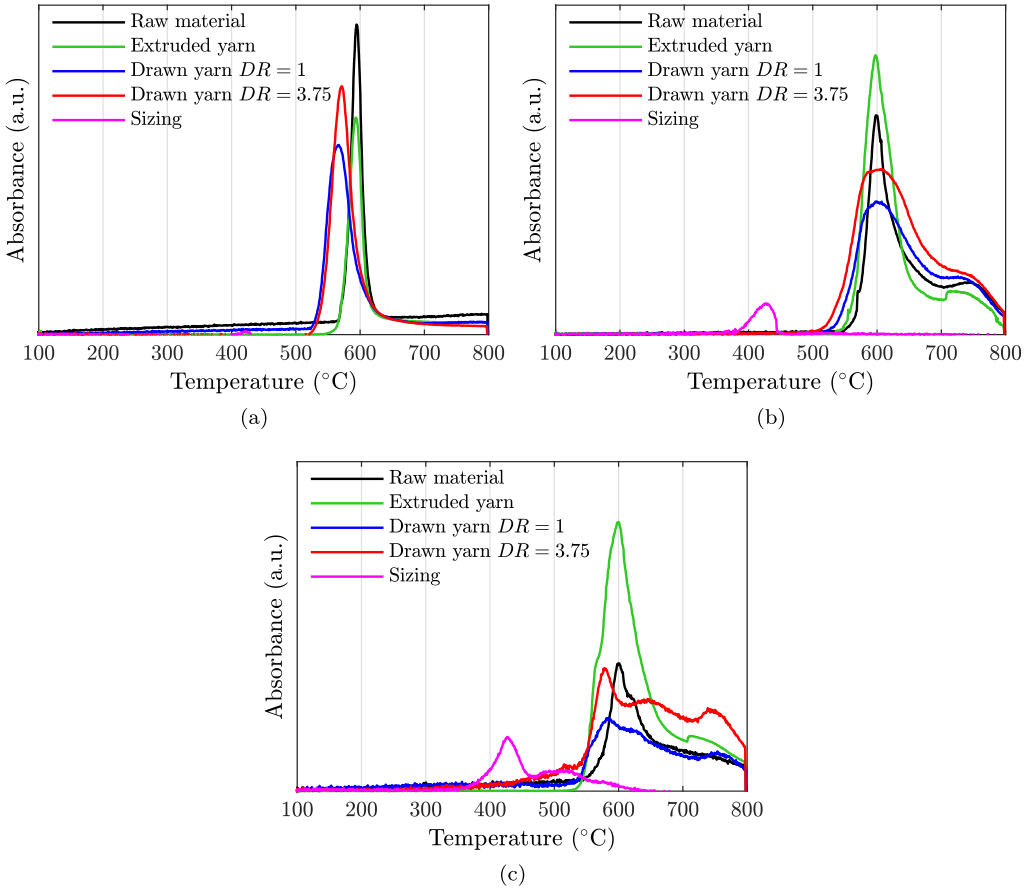

Fig. 9. Peak intensity profiles of the main degradation products of PEEK (a) Phenol (b) Carbon monoxide and (c) Carbon dioxide, during thermogravimetric analysis at 10 °C min^{-1}.

a double peak. This confirms that several steps are involved in the thermal decomposition mechanism of PEEK, as described in the literature [16].

It can be noticed that for the extruded yarn, the peak maximum is not shifted but the peak onset for all degradation products is 10 to 20 °C lower than that of the raw material. In addition, whatever the by-product, the peaks for raw and extruded PEEK have similar shapes. The absorbance peaks that correspond to the degradation steps have for both materials the same maximum temperature regardless of the by-product. This indicates that the extrusion step of the melt spinning process caused slightly earlier degradation without changing its chemical process. Extrusion is therefore likely to have initiated formation of radicals by chain breakage.

For the drawn yarns, regardless of their draw ratio, the same changes can be observed on the absorbance profiles, which indicates that sizing is responsible for modifications of the degradation process. The onset of absorbance peaks is significantly shifted to temperatures 25 to 45 °C lower than those of the raw material, leading to broader absorbance peaks. For phenols and carbon dioxide, this onset shift induces a distinct shift in the maximum of the absorbance peaks. For carbon monoxide, the maximum absorbance occurs at the same temperature as for the raw and extruded material, but the double peak shape indicates that the chemical modifications occur over a broader temperature range, suggesting a more gradual degradation process.

However, for carbon dioxide, the peak shape of the drawn yarns is significantly modified compared to the raw material. Instead of a double peak, the absorbance profile exhibits a triple peak, suggesting a change in decomposition mechanisms compared to the raw material. This particular peak shape that appears is relatively close to that of the sizing. It is therefore likely that the degradation by-products of sizing are involved in PEEK degradation mechanisms. In particular, it appears that carbonization that occurs above 750 °C is affected, with an intense carbon dioxide absorbance peak at about 780 °C [23,24].

These results show that, although the same decomposition products are identified, thermal degradation of PEEK is modified due to melt spinning processing. Extrusion appears to induce only a slightly earlier degradation process, while sizing applied to the surface of the drawn yarns appears to modify the degradation mechanisms with modifications occurring at lower temperatures. Nevertheless, no significant effect of the draw ratio on the degradation mechanisms could be detected with these techniques.

In this study, the products formed during sizing decomposition and the products resulting from their interaction with PEEK could not be identified due to the low quantity of sizing on the yarn surface (1.5% in mass). Further analyses with larger amount of additives will be required in order to identify the chemical process of PEEK decomposition in presence of additives. The nature of the sizing also should be investigated to better understand the interaction of PEEK with its environment.

4. Conclusion

The influence of different melt spinning parameters on the stability, thermal and rheological properties of poly(ether ether ketone) and its degradation process was analyzed using various experimental techniques. To do so, yarns collected at different stages of melt spinning were characterized and compared with raw PEEK: extruded yarns collected in the cooling chamber before being sized and drawn, and drawn yarns corresponding to yarns that were extruded, sized and drawn at different draw ratios.

PEEK degradation has been identified on the different yarns. As widely described in the literature, this degradation induces a decrease of the crystallization temperature and an increase of the viscosity in the molten state. This degradation is irreversible and can be a limiting factor in the processability of thermoplastic composite preforms.

The results show that the melt spinning operation has a significant effect on the PEEK properties. First, the extrusion affects the crystallization temperature and viscosity. It shifts slightly the beginning of degradation at lower temperatures without changing the decomposition process.

On the contrary, the drawn yarns have higher degradation kinetics than that of the raw PEEK and the extruded yarn. In addition, the TGA coupled with infrared spectroscopy suggests that sizing modifies PEEK degradation mechanisms due to an interaction of sizing by-products with PEEK. In addition, the draw ratio seems to induce different sizing ratio causing different degradation kinetics.

Further work should be carried out to investigate the effect of the chemical nature and stability of sizing on PEEK degradation.

CRediT author statement

Lisa Feuillerat and Carole Aubry performed the experiments. All authors interpreted the results. Lisa Feuillerat and Olivier De Almeida wrote the manuscript with the support of Jean-Charles Fontanier, Fabrice Schmidt, Carole Aubry and Pascal Rumeau. All authors provided critical comments and helped to shape the research, analysis and manuscript.

Declaration of Competing Interest

The authors declare that they have no known competing financial interests or personal relationships that could have appeared to influence the work reported in this paper.

Acknowledgments

The authors thank the Region Occitanie for their financial support in this project. The authors wish to thank the IFTH for their support in the melt spinning and TGA-FTIR characterizations. The authors wish also to thank Marion Carrier and Justine Arocas for their support on py-GC–MS/FID experiments, which were supported by the ANR funding of the PYROKINE project (ANR-18-MPGA-0013).

References

[1] A.M. Díez-Pascual, J. Guan, B. Simard, M.A. Gómez-Fatou, Poly(phenylene sulphide) and poly(ether ether ketone) composites reinforced with single-walled carbon nanotube buckypaper: I - Structure, thermal stability and crystallization behaviour, Compos. Part A 43 (6) (2012) 997–1006, doi:10.1016/j.compositesa.2011.11.002.

[2] G. Sala, D. Cutolo, Heated chamber winding of thermoplastic powder-impregnated composites: part 1. Technology and basic thermochemical aspects, Compos. Part A 27 (5) (1996) 387–392, doi:10.1016/1359-835X(95)00035-Z.

[3] Z. Xu, M. Zhang, S. Gao, G. Wang, S. Zhang, J. Luan, Study on mechanical properties of unidirectional continuous carbon fiber-reinforced PEEK composites fabricated by the wrapped yarn method, Polym. Compos. 40 (1) (2019) 56–69, doi:10.1002/pc.24600.

[4] V. Goud, R. Alagirusamy, A. Das, D. Kalyanasundaram, Influence of various forms of polypropylene matrix (fiber, powder and film states) on the flexural strength of carbon-polypropylene composites, Compos. Part B 166 (May 2018) (2019) 56–64, doi:10.1016/j.compositesb.2018.11.135.

[5] N. Bernet, V. Michaud, P.E. Bourban, J.A.E. Manson, Commingled yam composites for rapid processing of complex shapes, Compos. Part A 32 (11) (2001) 1613–1626, doi:10.1016/S1359-835X(00)00180-9.

[6] L. Feuillerat, O. De Almeida, J.-C. Fontanier, F. Schmidt, Effect of poly(ether ether ketone) degradation on commingled fabrics consolidation, Compos. Part A 149 (2021) 106482, doi:10.1016/j.compositesa.2021.106482.

[7] J.N. Hay, D.J. Kemmish, Thermal decomposition of poly(aryl ether ketones), Polymer 28 (12) (1987) 2047–2051, doi:10.1016/0032-3861(87)90039-5.

[8] M. Day, T. Suprunchuk, J.D. Cooney, D.M. Wiles, Thermal degradation of poly(aryl-ether-ether-ketone) (PEEK): a differential scanning calorimetry study, J. Appl. Polym. Sci. 36 (28274) (1988) 1097–1106, doi:10.1002/app.1988.070360510.

[9] M. Day, J.D. Cooney, D.M. Wiles, The thermal stability of poly(aryl-ether ether-ketone) as assessed by thermogravimetry, J. Appl. Polym. Sci. 38 (29850) (1989) 323–337, doi:10.1002/app.1989.070380214.

[10] A. Jonas, R. Legras, Thermal stability and crystallization of poly(aryl ether ether ketone), Polymer 32 (15) (1991) 2691–2706, doi:10.1016/0032-3861(91)90095-Z.

[11] K. Cole, I. Casella, Fourier transform infra-red spectroscopic study of thermal degradation in poly(ether ether ketone)-carbon composites, Polymer 34 (4) (1993) 740–745, doi:10.1016/0032-3861(93)90357-G.

[12] V. Myllärі, T.P. Ruoko, J. Vuorinen, H. Lemmetyinen, Characterization of thermally aged polyetheretherketone fibres - mechanical, thermal, rheological and chemical property changes, Polym. Degrad. Stab. 120 (2015) 419–426, doi:10.1016/j.polymdegradstab.2015.08.003.

[13] A. Deignan, W.F. Stanley, M.A. McCarthy, Insights into wide variations in carbon fibre/polyether-ether-ketone rheology data under automated tape placement processing conditions, J. Compos. Mater. (2017) 1–16, doi:10.1177/0021998317740733.

[14] M.I. Martín, F. Rodríguez-Lence, A. Güemes, A. Fernández-López, L.A. Pérez-Maqueda, A. Perejón, On the determination of thermal degradation effects and detection techniques for thermoplastic composites obtained by automatic lamination, Compos. Part A 111 (2018) 23–32, doi:10.1016/j.compositesa.2018.05.006.

[15] A. Pascual, M. Toma, P. Tsotra, M.C. Grob, On the stability of PEEK for short processing cycles at high temperatures and oxygen-containing atmosphere, Polym. Degrad. Stab. 165 (2019) 161–169, doi:10.1016/j.polymdegradstab.2019.04.025.

[16] P. Patel, T.R. Hull, R.W. McCabe, D. Flath, J. Grasmeder, M. Percy, Mechanism of thermal decomposition of poly(ether ether ketone) (PEEK) from a review of decomposition studies, Polym. Degrad. Stab. 95 (5) (2010) 709–718, doi:10.1016/j.polymdegradstab.2010.01.024.

[17] E. Courvoisier, Y. Bicaba, X. Colin, Multi-scale and multi-technique analysis of the thermal degradation of poly(ether ether ketone), Polym. Degrad. Stab. 151 (2018) 65–79, doi:10.1016/j.polymdegradstab.2018.03.001.

[18] G. Da Cunha Vasconcelos, R.L. Mazur, B. Ribeiro, E.C. Botelho, M.L. Costa, Evaluation of decomposition kinetics of poly (ether-ether-ketone) by thermogravimetric analysis, Mater. Res. 17 (1) (2014) 227–235, doi:10.1590/S1516-14392013005000202.

[19] O. De Almeida, L. Feuillerat, V. Nouri, K. Choquet, Influence of composite preform fabrication on the integrity of poly-aryl-ether-ketone matrices, J. Appl. Polym. Sci. 138 (30) (2021) 1–15, doi:10.1002/app.50719.

[20] R. Phillips, T. Glauser, J.A.E. Månson, Thermal stability of PEEK/carbon fiber in air and its influence on consolidation, Polym. Compos. 18 (4) (1997) 500–508, doi:10.1002/pc.10302.

[21] C.-M. Chan, S. Venkatraman, Crosslinking of poly(arylene ether ketone)s 1. Rheological behavior of the melt and mechanical properties of cured resin, J. Appl. Polym. Sci. 32 (7) (1986) 5933–5943, doi:10.1002/app.1986.070320722.

[22] T. Choupin, B. Fayolle, G. Régnier, C. Paris, J. Cinquin, B. Brulé, Macromolecular modifications of poly(etherketoneketone) (PEKK) copolymer at the melting state, Polym. Degrad. Stab. 155 (2018) 103–110, doi:10.1016/j.polymdegradstab.2018.07.005.

[23] A. Ramgobin, G. Fontaine, S. Bourbigot, A case study of polyether ether ketone (I): investigating the thermal and fire behavior of a high-performance material, Polymers 12 (8) (2020) 1789, doi:10.3390/polym12081789.

[24] C.J. Tsai, L.H. Perng, Y.C. Ling, A study of thermal degradation of poly(aryl-ether-ether-ketone) using stepwise pyrolysis/gas chromatography/mass spectrometry, Rapid Commun. Mass Spectrom. 11 (18) (1997) 1987–1995, doi:10.1002/(SICI)1097-0231(199712)11:18<1987::AID-RCM100>3.0.CO;2-Q.